RSC Advances

PAPER

View Article Online
View Journal | View Issue

Cite this: *RSC Adv.*, 2017, **7**, 32094

Mn^{4+} doped fluorotitanate phosphors: synthesis, optical properties and application in LED devices†

Qiang Zhou,[a] Huiying Tan,[a] Qiuhan Zhang,[a] Nan Wang,[a] Qianwen Wei,[a] Zhengliang Wang,*[a] Meizhu Rong[b] and Qin Wang*[b]

Received 18th April 2017
Accepted 18th June 2017

DOI: 10.1039/c7ra04369d

rsc.li/rsc-advances

In this work, we report an optimized cation exchange route for the production of a narrow-band $A_2TiF_6:Mn^{4+}$ (A = K, Na and Cs) red emitting phosphor using a small amount of non-toxic HAc solution instead of volatile and corrosive HF liquid. The crystal structure, morphology and doping amount of the $A_2TiF_6:Mn^{4+}$ products were characterized by powder X-ray diffraction (XRD), scanning electron microscopy (SEM), energy-dispersive X-ray spectroscopy (EDS) and atomic absorption spectrophotometry (AAS) in detail. The influence of the molar ratio of the raw materials, HAc concentration and reaction time on the photoluminescence behavior has been systematically investigated. Moreover, the role of HAc in the formation process is discussed in detail. By revealing its application in white light-emitting diodes (WLEDs) with tunable chromaticity coordinates and correlated color temperature, we confirm that the substitution of HAc for HF will increase the large scale production feasibility of the $A_2TiF_6:Mn^{4+}$ red phosphor for the WLED industry.

1. Introduction

In October 2014, Isamu Akasaki, Hiroshi Amano and Shuji Nakamura jointly won the Nobel Prize in Physics because of their successful and creative work in "the invention of efficient blue light-emitting diodes which has enabled bright and energy-saving white light sources" from the early 1990s.[1] Bright blue light beams emitted from blue LED chips can be absorbed by a yellow phosphor to produce white light.[2,3] Nowadays, the most popular commercial yellow phosphor, yttrium aluminum garnet (YAG, $Y_3Al_5O_{12}:Ce^{3+}$), has been widely used as the fundamental manufacturing constituent in the white light-emitting diode (WLED) illumination industry.[4,5] However, the scarcity of red light makes the white light dazzling and uncomfortable to people's eyes, which results from its high correlated color temperature (CCT, T_c > 4500 K) and low color rendering index (CRI, R_a < 80).[6,7] To overcome this drawback, considerable efforts have been devoted to exploring Mn^{4+} doped oxide and fluoride red phosphors, in which the energy levels of Mn^{4+} split and a distinct $^2E_g \rightarrow {}^4A_{2g}$ transition occurs.[8,9] This is why Mn^{4+} doped phosphors emit red light under blue light illuminations. Two typical examples are $Mg_2TiO_4:Mn^{4+}$ and $K_2TiF_6:Mn^{4+}$ phosphors. Merging them with YAG powders, cold white light will be balanced to warm. However, the emissions of $Mg_2TiO_4:Mn^{4+}$ located between 650 and 720 nm, which are too far red-shifted for high luminous efficiency warm WLEDs. Therefore, a number of research attentions have been paid on Mn^{4+} doped fluoride phosphors, since their broad excitation and intense emission properties in the blue and red regions.[10]

Recently, a variety of methods have been proposed to fabricate valance-stable Mn^{4+}/Mn^{6+} doped red phosphors.[11] Particularly for the preparation of Mn^{4+} doped hexa-fluorotitanate phosphor, the group of Chen fabricated $K_2TiF_6:Mn^{4+}$ red phosphor through an ion exchange method between K_2MnF_6 and K_2TiF_6 in HF solution.[12] Pan and her colleagues demonstrated the synthesis of $K_2TiF_6:Mn^{4+}$ and $BaTiF_6:Mn^{4+}$ red phosphors in high-concentrated HF acid reaction medium.[13,14] Xu and his co-workers prepared $K_2TiF_6:Mn^{4+}$ product by a two-step co-precipitation approach in HF solution.[15] In our previous work, we also prepared $Na_2TiF_6:Mn^{4+}$ and $Cs_2TiF_6:Mn^{4+}$ red phosphors in 40% HF solution.[16,17] Despite these successes, it should be noted that all of these approaches employed an excess amount of corrosive HF solution in the preparation process, in order to synthesize high brightness fluorotitanate red phosphors. That is because high HF concentration is favorable for the formation of $[MnF_6]^{2-}$ group.[18] However, taking safe operation and environmental protection during the preparation process into account, it appears very urgent to develop a safe and environmental friendly solvent as the

[a]*Key Laboratory of Comprehensive Utilization of Mineral Resource in Ethnic Regions, Joint Research Centre for International Cross-border Ethnic Regions Biomass Clean Utilization in Yunnan, School of Chemistry and Environment, Yunnan Minzu University, Kunming, 650500, P. R. China. E-mail: wangzhengliang@foxmail.com*

[b]*College of Chemistry and Chemical Engineering, Yunnan Normal University, Kunming, 650500, P. R. China. E-mail: wangqinynnu@163.com*

† Electronic supplementary information (ESI) available: Details to the XRD patterns of $K_2TiF_6:Mn^{4+}$ product prepared from different reaction medium, the DRS, EDS, decay and TG results of the optimum $K_2TiF_6:Mn^{4+}$, PL properties of $Cs_2TiF_6:Mn^{4+}$ and $Na_2TiF_6:Mn^{4+}$, WLED performance and corresponding CIE chromaticity diagram data. See DOI: 10.1039/c7ra04369d

reaction medium to substitute HF solution for the fabrication of Mn^{4+} doped fluoride red phosphors, to avoid the extensive usage of HF acid and the resulting pollution.

In this work, we demonstrate an optimized ion exchange procedure for the fabrication of Mn^{4+} doped fluorotitanate ($A_2TiF_6:Mn^{4+}$, A = K, Na and Cs) red phosphors, with the employment of green HAc acid instead of corrosive HF acid. The reaction conditions, optical properties and performance are carefully investigated in detail. All of the obtained products can present wide blue light absorption, sharp red line emission, excellent thermal stability and high color purity characteristics, implying HAc would be an efficient and feasible solvent for large scale production of $A_2TiF_6:Mn^{4+}$ red phosphor for WLED application.

2. Experimental

2.1. Materials

All source materials in this work, including potassium hydrogen bifluoride (KHF_2), potassium permanganate ($KMnO_4$), hydrogen peroxide (H_2O_2, 30%), hexafluorotitanic acid (H_2TiF_6, 50%), potassium fluoride (KF), sodium fluoride (NaF), cesium fluoride (CsF), glacial acetic acid (HAc, 99.5%), acetone and absolute alcohol were of analytical grade and used as obtained without any further purification. The YAG yellow phosphor was commercially purchased from Shenzhen Quanjing Photon Co. Ltd., China.

2.2. Materials preparation

Different from other ion exchange reaction occurred in corrosive HF solution, in this work, the formation of $A_2TiF_6:Mn^{4+}$ products were carried out in green HAc solution. In a typical synthesis, 2.0 mmol H_2TiF_6 was added into 5.0 ml HAc solution with magnetic stirring in a 50 ml plastic beaker. It should be noted that HAc solution consists of a certain amount of glacial acetic acid and deionized water. Then 0.1 mmol K_2MnF_6 was put into the above mixture solution, followed by 5 mmol KF was added into the colorless transparent solution. After 30 min magnetic stirring, the precipitation was collected, washed with absolute alcohol for three times and dried at 60 °C for 2.0 h. For comparison, $A_2TiF_6:Mn^{4+}$ products were prepared with different initial molar ratios between H_2TiF_6 and K_2MnF_6 (denoted as TMR, ratios are 5, 10, 15, 20, 30 and 40), and different glacial acetic acid volume of 0, 0.05, 0.1, 0.5, and 1.0 ml. Additionally, the preparation of Mn^{4+} precursor K_2MnF_6 is according to Bode's method.[19]

2.3. Fabrication of LEDs

The as-prepared $A_2TiF_6:Mn^{4+}$ red phosphor, commercially purchased YAG yellow phosphor and blue GaN chip were used to fabricate WLED devices. Different amount of $A_2TiF_6:Mn^{4+}$ and YAG phosphors were mixed with epoxy resin thoroughly, followed by a coating process of phosphor-epoxy resin mixture on the surface of GaN chip. The obtained WLED devices were operated and measured under a forward current of 20 mA.

2.4. Material characterization

Powder X-ray diffraction (XRD, D8 Advance, Bruker, Germany) equipped with graphite monochromatized Cu Kα radiation (λ = 0.15406 nm) was used to measure the crystal structure of the as-prepared $A_2TiF_6:Mn^{4+}$ product, which was operated at 40 kV and 20 mA from 15° to 70°. Surface morphology was observed from a scanning electron microscopy (SEM, FEI Quanta 200 Thermal FE Environment scanning electron microscopy) with an attached energy-dispersive X-ray spectrometer (EDS). Compositional analysis was performed on a Shimadzu AA-6300 atomic absorption spectrophotometer (AAS). The Diffuse Reflectance Ultraviolet-Visible spectra (DRS) and decay curve were recorded on an Cary 5000 UV-Vis-NIR spectrophotometer and an Edinburgh FLS920 combined fluorescence lifetime and steady state spectrometer with a 450 W xenon lamp and 60 W μF flash lamp, respectively. PLE and PL properties were examined on a Cary Eclipse FL1011M003 (Varian) spectrofluorometer, which employs a xenon lamp as the excitation source. A high accurate array spectrometer (HSP6000) was used to investigate the performance of WLED devices.

3. Results and discussion

It has been reported previously that during the formation process of $A_2TiF_6:Mn^{4+}$ phosphor, HF acid plays not only an important F source, but also prevents the hydrolysis of $[MnF_6]^{2-}$ group. Nevertheless, the characteristics of hypertoxicity and potential fatal damage to human body make the reaction medium HF acid urgently to be replaced in the synthesis process. The group of Wang has done some useful explorations in this field.[20,21] In this work, we aimed to use simple inorganic/organic acid as reaction medium during the ion exchange process. Therefore, typical normal acids, such as HNO_3, H_2SO_4, H_3PO_4, HCl, and HAc were investigated and the results were displayed in Fig. S1a (see ESI†). Obviously, no matter what kinds of acid was used, $K_2TiF_6:Mn^{4+}$ product was prepared successfully. However, it should be noted that with the same volume amount of acid in reaction system, the obtained $K_2TiF_6:Mn^{4+}$ products exhibit different emission intensity (Fig. S1b†). It can be clearly observed that $K_2TiF_6:Mn^{4+}$ product prepared from strong acidic environment such as H_2SO_4, HCl and HNO_3, presents weaker PL intensity than that of HAc. Taking safe operation and environmental friendly into account, HAc is chosen as the reaction medium for the following preparation of $K_2TiF_6:Mn^{4+}$ product.

Fig. 1a shows the representative XRD pattern of the $K_2TiF_6:Mn^{4+}$, $Na_2TiF_6:Mn^{4+}$ and $Cs_2TiF_6:Mn^{4+}$ products, along with the standard diffraction cards of their corresponding hosts. Clearly from curve (i), all the diffraction peaks match perfectly with the JCPDS card of K_2TiF_6 (No. 08-0488), which belongs to the hexagonal structure (ICSD No. 24659) with $P\bar{3}m1$ space group. In this compound, Ti^{4+} ion is located at the center of the octahedral $[TiF_6]^{2-}$ group. Since the ionic radius of Mn^{4+} (r = 0.530 Å) is close to that of Ti^{4+} (r = 0.605 Å) ion and their coordination number are same (CN = 6), the Mn^{4+} ions would occupy the octahedral core sites of Ti^{4+} in this compounds,

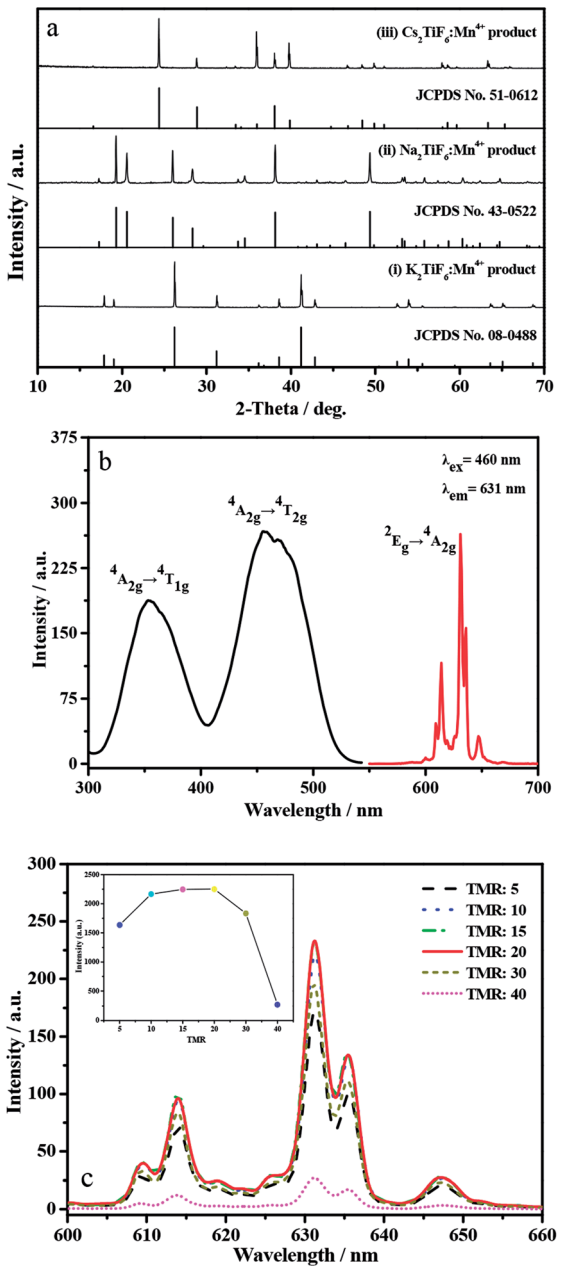

Fig. 1 (a) XRD patterns of (i) $K_2TiF_6:Mn^{4+}$, (ii) $Na_2TiF_6:Mn^{4+}$ and (iii) $Cs_2TiF_6:Mn^{4+}$. (b) PLE and PL spectra of $K_2TiF_6:Mn^{4+}$ product prepared with TMR of 20. (c) PL spectra of $K_2TiF_6:Mn^{4+}$ product prepared with different TMRs. The inset figure of (c) shows the relationship between TMR and the relative integral emission intensity.

resulting in the replacement of Mn^{4+} for Ti^{4+} in the center of $[TiF_6]^{2-}$ octahedron. Additionally, curve (ii) and (iii) also suggest that the obtained $Na_2TiF_6:Mn^{4+}$ and $Cs_2TiF_6:Mn^{4+}$ products exhibit pure-phases.

Fig. 1b displays the PLE and PL spectra of the above $K_2TiF_6:Mn^{4+}$ product. In PLE spectrum, two broad excitation bands peaking at 353 and 460 nm can be clearly observed, which are ascribed to the spin-allowed transitions of Mn^{4+} from ground state $^4A_{2g}$ to excited states $^4T_{1g}$ and $^4T_{2g}$ respectively.[21] The latter one, peaking at 460 nm, not only accords with the strongest adsorption peak of DRS result in Fig. S2 (ESI†), but also exhibits broader full width at half maximum (FWHM, 68 nm) than that of blue GaN chip emission (~20 nm). This reveals the $K_2TiF_6:Mn^{4+}$ phosphor can absorb blue light emissions from GaN chip efficiently. In PL part, red emissions are resulted from the spin-forbidden d–d transition of Mn^{4+} from ^2E_g to $^4A_{2g}$. The five peaks locating at 614, 619, 631, 635, and 647 nm are originated from the anti-Stokes ν_4, ν_6 and Stokes ν_4, ν_6 and ν_3 vibronic emissions.[22] Among the five peaks, the strongest one locates at 631 nm.

Table 1 AAS results of $K_2TiF_6:Mn^{4+}$ phosphors prepared with different TMRs

Samples	TMR	Doping amount of Mn^{4+} (mol%)
i	5	8.84
ii	10	6.41
iii	15	5.16
iv	20	2.84
v	30	1.99
vi	40	1.42

Fig. 1c shows the PL spectra of $K_2TiF_6:Mn^{4+}$ phosphors prepared with different TMRs. Apparently, the emission intensity firstly increases and then decreases with the TMR from 5 to 40. When TMR is 20, the obtained $K_2TiF_6:Mn^{4+}$ phosphor emits the strongest red light. This may because higher TMR value means lower Mn^{4+} concentration and less doping amount. So, when the TMR dropped from 40 to 20, the doping amount of Mn^{4+} contrarily rose up from 1.42% to 2.84%, which resulting in an increase trend of the PL intensity. Continually decreasing TMR from 20 to 5, more and more Ti^{4+} ions were substituted until the concentration quenching phenomenon occurred, which leads to the following decrease tendency of the PL intensity. This is in agreement with the doping amount of Mn^{4+} in these six products, according the results of AAS (Table 1). Actually, in the case of other phosphors $Na_2TiF_6:Mn^{4+}$ and $Cs_2TiF_6:Mn^{4+}$, the same rise–fall phenomenon was also observed (Fig. S3 in ESI†). In a word, at this TMR of 20, the obtained $K_2TiF_6:Mn^{4+}$ phosphor emits the brightest red light.

Fig. 2a shows the SEM image of the above $K_2TiF_6:Mn^{4+}$ product. It clearly exhibits that the particles have a particulate morphology with an apparent large size of *ca.* 40 μm. Additionally, we can clearly observe the smooth surfaces, clear edges and corners on these particles, implying the sample has been well crystallized into crystals.[23] From the corresponding EDS spectrum, the elements of F, Ti, K, and Mn, as well the absence of O element, can be clearly recognized (Fig. S4†). This result suggests that the Mn element has been successfully doped into the crystal structure of K_2TiF_6 matrix to occupy the lattice site of Ti, and no MnO_2 was produced during the entire preparation process. This result is line with the above PL results. Using HAc solution as reaction medium, $Na_2TiF_6:Mn^{4+}$ and $Cs_2TiF_6:Mn^{4+}$ products were also obtained and presented the same characteristic of particulate morphologies (Fig. 2d and e). Moreover, observed by naked eyes, the $K_2TiF_6:Mn^{4+}$ sample shows

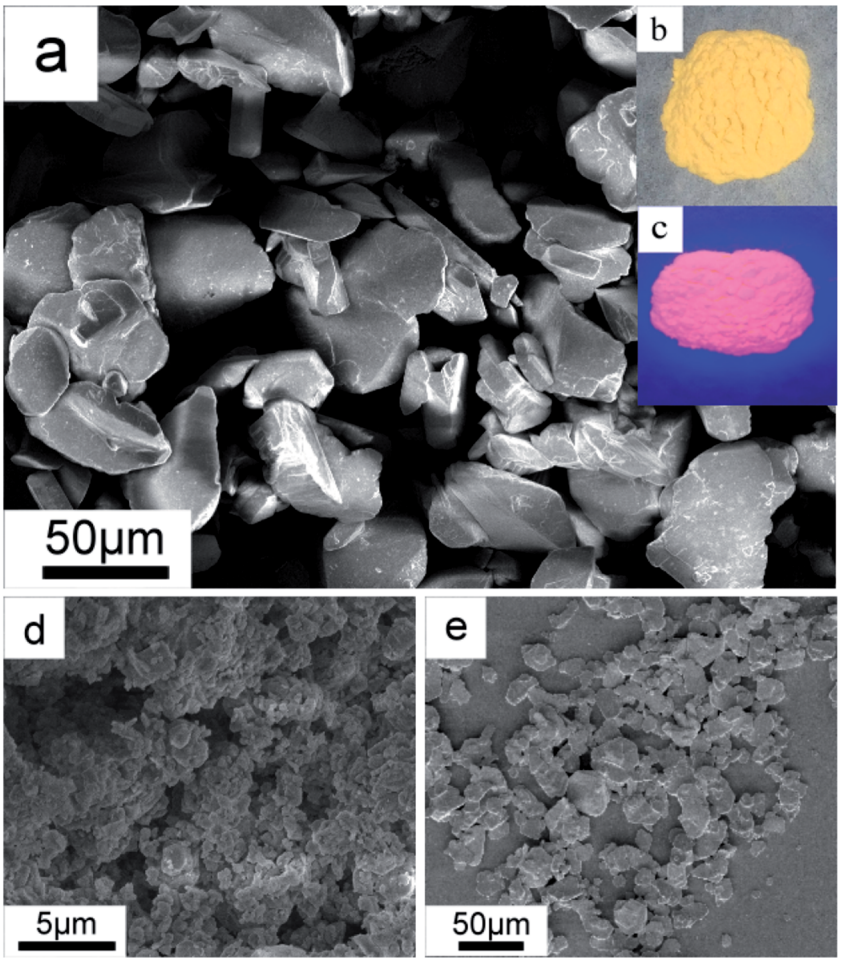

Fig. 2 $K_2TiF_6:Mn^{4+}$ red phosphor: (a) SEM image with typical photos illuminated under (b) natural and (c) 460 nm blue light. (d) and (e) are SEM images of $Na_2TiF_6:Mn^{4+}$ and (c) $Cs_2TiF_6:Mn^{4+}$ products.

a striking yellow color under natural light illumination (Fig. 2b) whist emits brilliant red light under blue light (460 nm) illumination (Fig. 2c).

As it known, for a product prepared using this wet-chemical synthesis route, it is essential to investigate the influence of some general reaction conditions on the optical properties. Firstly, the influence of HAc concentration on the PL property of $K_2TiF_6:Mn^{4+}$ phosphor was investigated and shown in Fig. S5.† Similar to the above result, all the $K_2TiF_6:Mn^{4+}$ phosphors emit red light as well. Moreover, HAc concentration of 0 means the reaction solvent is deionized water, in which $[MnF_6^{2-}]$ may hydrolyze and produce impurities, leading to its poor emission intensity. Increasing HAc concentration from 0 to 2%, more and more H^+ was produced to suppress the hydrolysis of $[MnF_6^{2-}]$ group. At 2%, the obtained $K_2TiF_6:Mn^{4+}$ phosphor emits the brightest red light. Keeping the pace of addition, excessive HAc molecules in reaction solution resulted in the less generation of H^+ and emission intensity reduction of $K_2TiF_6:Mn^{4+}$ phosphor. The relationship between HAc volume and the relative integral emission intensity of $K_2TiF_6:Mn^{4+}$ phosphor is illustrated in the inset of Fig. S5.†

Secondly, the effect of synthesis time on the PL properties of $K_2TiF_6:Mn^{4+}$ red phosphor is investigated and the results are shown in Fig. 3. It is very clear that the shapes of these PL

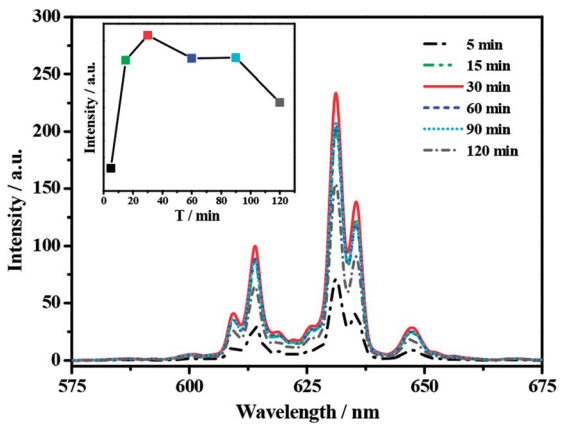

Fig. 3 PL spectra for $K_2TiF_6:Mn^{4+}$ products prepared with different reaction time (λ_{ex} = 460 nm). The insert figure is the relationship between reaction time and relative integral emission intensity.

spectra are similar to above. As illustrated above, they are attributed to the spin-forbidden transition of Mn^{4+} from ^2E_g to $^4A_{2g}$. Secondly, the ZPL emission is hardly to be observed. This is exactly the same as that of Cs_2TiF_6:Mn^{4+}, but completely different with that of Na_2TiF_6:Mn^{4+}, in which ZPL emission is the main part (Fig. S6†).[24] Moreover, it is obvious that the emission intensity can be enhanced by increasing the reaction time from 5 to 30 min, which may be resulted from the improved doping amount of Mn^{4+}. Further prolongation of reaction time causes a downward trend of emission intensity. It is possible that too much Ti^{4+} ions have been substituted by Mn^{4+} ions, which resulting in the concentration quenching of Mn^{4+} in K_2TiF_6 host.[25] The same quenching phenomenon also can be observed from the time-dependent PL spectra of Cs_2TiF_6:Mn^{4+} and Na_2TiF_6:Mn^{4+} phosphors (Fig. S6†). The relationship between reaction time and the relative integral emission intensity of K_2TiF_6:Mn^{4+} phosphor is presented in the inset figure of Fig. 3.

Therefore, on the basis of the above discussion, we can conclude that HAc solution is an acceptable, safe using and environmental friendly reaction solvent for the ion exchange formation of K_2TiF_6:Mn^{4+} red phosphor. The corresponding optimum reaction conditions are: TMR is 20, 2% HAc solution, reacted at room temperature for only 30 min. Consequently, this optimized sample, in which the doping amount of Mn^{4+} is 2.84 mol%, was chosen for the following decay curve, thermal behavior, temperature-dependence and WLED performance investigations.

Fig. S7a† displays the PL decay curve of the emitting state ^2E_g of Mn^{4+} in the optimum K_2TiF_6:Mn^{4+} phosphor examined at room temperature. Obviously, this curve is well fitted into a single-exponential function with lifetime τ value of 5.71 ms. Thermal stability of this sample was examined on a thermogravimetric (TG) instrument. The result is shown in Fig. S7b† and two valleys can be clearly observed. In the former valley, a weak endothermic peak with weight loss about 5% at a temperature below 100 °C can be found, which is mainly attributed to the adsorbed moisture. The mass of the sample begins to be lost at 385 °C accompanied with an endothermic peak, which indicates that the phosphor decomposes at temperatures higher than 385 °C. Thus, the sample is thermally stable under ambient atmosphere for WLED applications.

The influence of temperature on the PL properties of the optimum K_2TiF_6:Mn^{4+} red phosphor at 20–180 °C under 460 nm blue light excitation was investigated and the representative results are presented in Fig. 4. Apparently, it can be clearly observed that with the temperature rising from 40 to 180 °C, the emission intensity exhibits a lower tendency because of the increasing non-radiative transition processes. Furthermore, with the temperature increasing, not only emission spectrum gradually becomes broader, but also the main emission peak positions exhibit swiftly red-shift. This is due to the expansion of unit cell and the enhancement of vibration modes of $[MnF_6]^{2-}$ octahedron in hot environment. This result is in agreement with the previous reports.[26,27] Furthermore, the relationship between temperature and integral emission intensity is inserted in Fig. 4, which displays considerable stability for K_2TiF_6:Mn^{4+} phosphor with working temperature increases from 20 to 120 °C. When the temperature is 120 °C, nearly 117% of the integral emission intensity can be achieved, compared with that at 20 °C. Up to 140 °C, the relative integral intensity still preserve about 107%. This can be attributable to the integral anti-Stokes emission intensity increased with temperature, whereas the integral Stokes emission intensity remained basically unchanged.[12]

As reported previously, the FWHM of the emission band for GaN chip in the blue-light region is about 20 nm, which is much narrower than that of the above K_2TiF_6:Mn^{4+} phosphor (~68 nm).[28] Additionally, they share the similar emission peak locations. This results in the K_2TiF_6:Mn^{4+} phosphor was chosen to cooperate with YAG yellow phosphor and GaN chip in a WLED device to possess warm white light. In this device, K_2TiF_6:Mn^{4+} and YAG phosphors can absorb the blue light emissions of GaN chip to illuminate bright red and yellow light respectively, in which the blue, yellow and red light can mix and possess warm white light to our eyes. Thus, from a practical point of view, it is

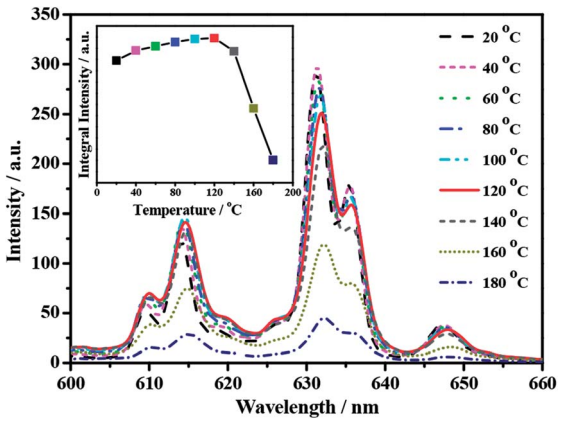

Fig. 4 Temperature-dependent emission spectra of K_2TiF_6:Mn^{4+} phosphor and relative intensity of emission spectrum by integrating the spectral area (λ_{ex} = 460 nm).

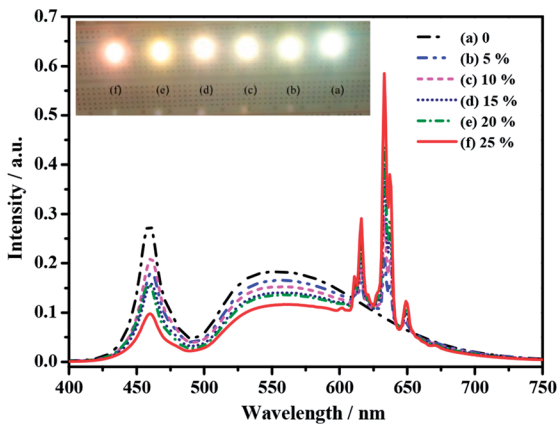

Fig. 5 Electroluminescent (EL) spectra and photographs of six LED devices recorded at 20 mA drive current.

necessary to investigate the optical performance of this WLED devices and the results were shown in Fig. 5, which is the electro-luminescent (EL) spectra of a series of LEDs fabricated by merging YAG, various amount of K_2TiF_6:Mn^{4+} and epoxy resin on blue GaN chips recorded at 20 mA drive current. Obviously, only with a single YAG component, the obtained white light exhibits weak emissions in the red region with high T_c (5139 K) and low R_a (71.8) with a super-excellent luminous efficiency (189.98 lm W^{-1}). After the introduction of K_2TiF_6:Mn^{4+}, obvious red light emission in the spectra can be observed. Increasing its addition amount from 0 to 25%, a noticeable stronger tone of the emitting red light can be observed. The chromaticity coordinates of these WLED devices are labeled in or close to the white light region in CIE 1931 color spaces as points of (a–f) in Fig. S9 in ESI.† Photographs of the lighting LEDs are shown in the insert image of Fig. 5. Their corresponding T_c, R_a and luminous efficiency data are compared listed in Table S1 in ESI.† The EL spectra reconfirm the sharp emission lines of K_2TiF_6:Mn^{4+} phosphor and more red components with lower CCTs. Furthermore, by adding K_2TiF_6:Mn^{4+} phosphor into the YAG powders with its addition amount from 0 to 25%, the T_c data dropped from 5139 to 2969 K and R_a improved from 71.8 to 94.1. In a word, the R_a and T_c of the warmest WLED are 94.1 and 2969 K whist keeping an excellent luminous efficiency of 156.04 lm W^{-1}. Moreover, introducing Na_2TiF_6:Mn^{4+} or Cs_2TiF_6:Mn^{4+} into the YAG system, obvious improvements on R_a and CCT level also can be obtained (Fig. S8, Tables S2 and S3 in ESI†).

4. Conclusions

In summary, we have developed a simplified and non-toxic ion exchange strategy for the formation of narrow-band red emitting A_2TiF_6:Mn^{4+} phosphors using HAc liquor as reaction solvent. The influence of synthesis conditions, including TMR, HAc concentration and reaction time on the PL properties of K_2TiF_6:Mn^{4+} product have been investigated in detail. Results show that the optimal TMR is 20, reacted in 2% HAc solution for 30 min, whist the optimal doping concentration of Mn^{4+} is 2.84 mol%. Because of these properties, by integrating these red phosphors with commercial YAG and commercial blue chip, we can observe warm white light with high CRI ($R_a = 94.1$), low CCT (T_c = 2969 K) and excellent luminous efficiency of 156.04 lm W^{-1} from WLED device working at 20 mA driven current and 5 V voltage.

Acknowledgements

We are gratefully acknowledge the financial supports from the National Natural Science Foundation of China (51662039 and 21661033), the Applied Basic Research Project of Yunnan Province (2014FB147), Graduate Innovation Foundation of Yunnan Minzu University (2015YJCXY277), Program for Innovative Research Team (in Science and Technology) in University of Yunnan Province (2011UY09) and Yunnan Provincial Innovation Team (2011HC008).

References

1 S. Nakamura, *Ann. Phys.*, 2015, **54**, 7770.
2 H. D. Nguyen, C. C. Lin and R. S. Liu, *Angew. Chem., Int. Ed.*, 2015, **54**, 10862.
3 W. T. Chen, H. S. Shen, R. S. Liu and J. P. Attfield, *J. Am. Chem. Soc.*, 2012, **134**, 8022.
4 E. H. Song, J. Q. Wang, S. Ye, X. F. Jiang, M. Y. Peng and Q. Y. Zhang, *J. Mater. Chem. C*, 2016, **4**, 2480.
5 Q. Zhou, Y. Y. Zhou, Y. Liu, L. J. Luo, Z. L. Wang, J. H. Peng, J. Yan and M. M. Wu, *J. Mater. Chem. C*, 2015, **3**, 3055.
6 C. C. Lin and R. S. Liu, *J. Phys. Chem. Lett.*, 2011, **2**, 1268.
7 L. L. Wei, C. C. Lin, Y. Y. Wang, M. H. Fang, H. Jiao and R. S. Liu, *ACS Appl. Mater. Interfaces*, 2015, **7**, 10656.
8 T. Takahashi and S. Adachi, *J. Electrochem. Soc.*, 2008, **155**, E183.
9 Y. K. Xu and S. Adachi, *J. Electrochem. Soc.*, 2011, **158**, J58.
10 J. H. Li, J. Yan, D. W. Wen, W. U. Khan, J. X. Shi, M. M. Wu, Q. Su and P. A. Tanner, *J. Mater. Chem. C*, 2016, **4**, 8611.
11 X. W. Zhang, Y. Li, C. X. Liao, Z. Chen and J. R. Qiu, *Nanotechnology*, 2017, **28**, 025604.
12 H. M. Zhu, C. C. Lin, W. Q. Luo, S. T. Shu, Z. G. Liu, Y. S. Liu, J. T. Kong, E. Ma, Y. G. Cao, R. S. Liu and X. Y. Chen, *Nat. Commun.*, 2014, **5**, 4312.
13 L. F. Lv, Z. Chen, G. K. Liu, S. M. Huang and Y. X. Pan, *J. Mater. Chem. C*, 2015, **3**, 1935.
14 X. Y. Jiang, Z. Chen, S. M. Huang, J. G. Wang and Y. X. Pan, *Dalton Trans.*, 2014, **43**, 9414.
15 F. Tang, Z. C. Su, H. G. Ye, M. Z. Wang, X. Lan, D. L. Phillips, Y. G. Cao and S. J. Xu, *J. Mater. Chem. C*, 2016, **4**, 9561.
16 Z. L. Wang, Y. Liu, Y. Y. Zhou, Q. Zhou, H. Y. Tan, Q. H. Zhang and J. H. Peng, *RSC Adv.*, 2015, **5**, 58136.
17 Q. Zhou, Y. Y. Zhou, Y. Liu, Z. L. Wang, G. Chen, J. H. Peng, J. Yan and M. M. Wu, *J. Mater. Chem. C*, 2015, **3**, 9615.
18 L. F. Lv, X. Y. Jiang, S. M. Huang, X. A. Chen and Y. X. Pan, *J. Mater. Chem. C*, 2014, **2**, 3879.
19 H. Bode, H. Jenssen and F. Bandte, *Angew. Chem.*, 1953, **65**, 304.
20 L. Huang, Y. W. Zhu, X. J. Zhang, R. Zou, F. J. Pan, J. Wang and M. M. Wu, *Chem. Mater.*, 2016, **28**, 1495.
21 Y. W. Zhu, L. Huang, R. Zou, J. H. Zhang, J. B. Yu, M. M. Wu, J. Wang and Q. Su, *J. Mater. Chem. C*, 2016, **4**, 5690.
22 X. Q. Li, X. M. Su, P. Liu, J. Liu, Z. L. Yao, J. J. Chen, H. Yao, X. B. Yu and M. Zhan, *CrystEngComm*, 2015, **17**, 930.
23 J. H. Oh, H. Kang, Y. J. Eo, H. K. Park and Y. R. Do, *J. Mater. Chem. C*, 2015, **3**, 607.
24 T. Arai and S. Adachi, *J. Appl. Phys.*, 2011, **110**, 063514.
25 C. X. Liao, R. P. Cao, Z. J. Ma, Y. Li, G. P. Dong, K. N. Sharafudeen and J. R. Qiu, *J. Am. Ceram. Soc.*, 2013, **96**, 3552.
26 L. L. Wei, C. C. Lin, M. H. Fang, M. G. Brik, S. F. Hu, H. Jiao and R. S. Liu, *J. Mater. Chem. C*, 2015, **3**, 1655.
27 M. Peng, X. Yin, P. A. Tanner, C. Liang, P. Li, Q. Zhang and J. Qiu, *J. Am. Ceram. Soc.*, 2013, **96**, 2870.
28 R. Kasa and S. Adachi, *J. Appl. Phys.*, 2012, **112**, 013506.